International Journal of Microwave and Wireless Technologies, 2017, 9(2), 327–334.
doi:10.1017/S1759078715001348

RESEARCH PAPER

Design of a CPW-fed UWB printed antenna with dual notch band using mushroom structure

TAPAN MANDAL[1] AND SANTANU DAS[2]

A coplanar waveguide-fed planar hexagonal monopole ultra-wideband antenna with dual-band rejection characteristics is proposed in this paper. The desired notch frequencies at 3.5 and 5.5 GHz are realized by incorporating mushroom structures. The input impedance and surface current distributions are used for analysis and explanation of the effects of mushroom cells. The prototype and proposed antennas are fabricated and tested. From the measured results, the proposed antenna provides an operating band of 2.81–14.32 GHz for 2 ≤ voltage standing wave ratio (VSWR), while the dual-band stop function is in the frequency bands of 3.3–3.7 GHz and 5.10–5.88 GHz. Moreover, the antenna model also exhibits constant group delay and linear phase in the pass band. The proposed antenna has appreciable gain and efficiency over the whole operating band except the notch bands.

Keywords: UWB, WLAN band, WiMAX band, CPW fed, mushroom

Received 13 May 2015; Revised 29 July 2015; Accepted 30 July 2015; first published online 2 September 2015

I. INTRODUCTION

Ultra-wideband (UWB) technology was approved by the Federal Communications Commission (FCC) since February 2002 [1]. As FCC rules, the authorized frequency range of UWB is 3.1–10.6 GHz for commercial wireless communications systems. In spite of large bandwidth (BW), several elegant advantages of UWB technology are low-power spectral density, high data rates, and high security. This kind of planer wideband antenna is designed using microstrip [2, 3] or coplanar waveguide (CPW) feeding line [3–7]. In particular, researchers and academicians pay much attention in CPW-fed antennas because of their several attractive features such as simple structure with single metallic layer, low cost, low radiation loss, and easy integration with microwave-integrated circuits [4–7]. However, it faces lot of challenges such as impedance matching, radiation stability, and electromagnetic interference problems (EMI). The EMI are quite serious problem for the UWB systems because there are some narrow bands within the UWB range for other communication. Therefore, it is desirable to design an UWB antenna with band-notch characteristics in order to avoid interference with the existing service bands such as Wireless Local Area Network (WLAN: IEEE 802.11a: 5.15–5.825 GHz) and Worldwide Interoperability for Microwave Access (WiMAX: IEEE 802.16:3.3–3.7 GHz).

However, several design methods have been proposed to produce the band notch in UWB. Among these approaches, band rejection characteristics are obtained by slots on metallic patch, feeder, ground plane, or using parasitic elements near the radiator [5–7]. For printed monopole antennas, the most familiar methods to achieve band-notch function are etching slots in various shapes [5, 6]. But many of them affect the radiation pattern due to perturbation of radiating element. Various types of electromagnetic band gap (EBG) structures have been used to enhance the gain [8], BW [9], and surface wave reduction [10]. Currently band-notch characteristics in the UWB frequency region have been described using mushroom-type EBG structures [11–16]. The stepped index resonators have been introduced within the UWB antenna body for the band-notch characteristics [17].

In this paper, a CPW-fed printed regular hexagonal monopole antenna (PRHMA) with WiMAX and WLAN band-notch characteristics has been proposed. The desired notch-band characteristics are obtained by incorporating mushroom structures. The resonant frequency and BW of the notch bands can be controlled by tuning the parameters of the mushroom structures. To evaluate the antenna performance method of moment based IE3D™ simulation software is used. A PRHMA with dual-band stop using mushroom structures has not been investigated in details so far. Besides, it has small size [4, 13, 14, 18], simple structure [4, 13, 14, 18–20] and shorter computation time for the optimization process [11–14, 16–18].

II. ANTENNA GEOMETRY AND DESIGN CONSIDERATION

A) UWB antenna geometry

The geometric configuration of the prototype antenna is presented in Fig. 1. It is printed on a substrate with dielectric

[1]Department of Information Technology, Government College of Engineering and Textile Technology, Serampore, Hooghly-712201, West Bengal, India
[2]Department of Electronics and Tele-Comm. Engineering, Indian Institute of Engineering Science and Technology, Shibpur, Howrah-711103, West Bengal, India
Corresponding author:
T. Mandal
Email: tapanmandal20@rediffmail.com

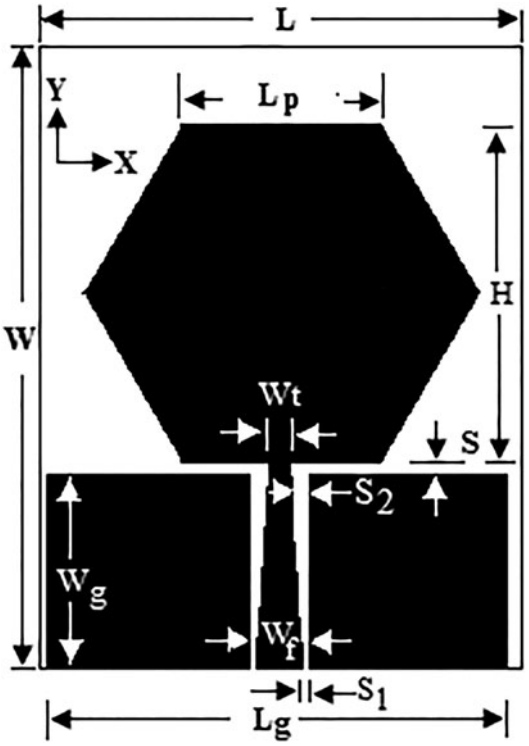

Fig. 1. Configuration of prototype of PRHMA.

constant (ε_r) of 4.4 and thickness (h) of 1.59 mm. It has a hexagonal patch, ground plane, and CPW-fed line on the same plane of the substrate. The radiating patch is connected by a tapered CPW line for good impedance matching. The dimensions are given in Table 1 to cover the UWB frequency range.

B) UWB antenna with WLAN and WiMAX band notch

To achieve the WiMAX stop band from the UWB operating band, a mushroom structure is introduced on the opposite side of radiating patch. In addition to this, WLAN stop band is realized by inserting a pair of mushroom structures at the underneath of ground plane. The mushroom cells are placed symmetrically with respect to fed line. A pair of mushroom cell is used to get strong rejection signal. All the parameters of the mushroom patches are shown in Fig. 2, which indicates the proposed antenna. The desired dimension values of the proposed antenna are shown in Table 1.

C) Equivalent-circuit model

The mushroom cell is via loaded metallic patch. The square structure play a role of capacitance and the shorting pin (via) is equivalent to the inductance at the notch band. An

Table 1. Dimensions of the proposed antenna.

Parameter	L	W	L_g	W_g	S	L_p	W_f	W_t	S_1
Dimension (mm)	32	48	28	13.5	1.35	13.6	4.4	4.1	0.4
Parameter	S_2	H	W_e	d_2	d_1	W_{e1}	d_3	$2r$	X
Dimension (mm)	0.55	23.5	7.1	0.15	0.75	4.5	0.05	0.4	0.5

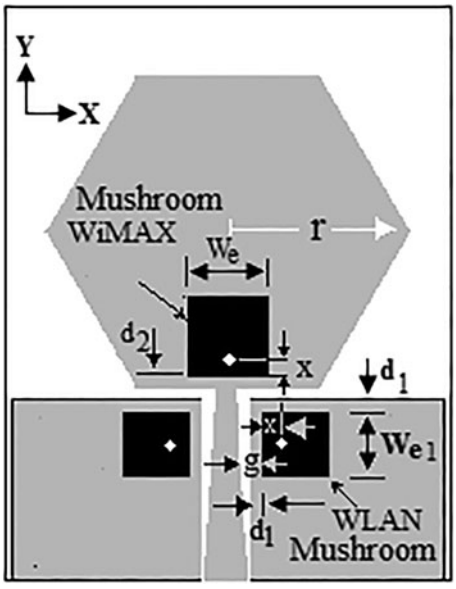

Fig. 2. Configuration of the proposed antenna.

equivalent-circuit model of the mushroom structure is presented in Fig. 3. The resonant frequency of the mushroom cell which is the center frequency of the notch band can be expressed as:

$$f_r = \frac{1}{2\pi\sqrt{L(C_o + C_1)}}, \tag{1}$$

where C_o represents the coupling capacitance between the mushroom structure and the feed line, while the capacitance C_1 is due to the voltage gradients between the patch and ground plane. The inductance L is generated by the current flowing through the shorting via. The desired notch frequency and notch BW can be obtained by tuning the values of inductance and capacitance mainly by fixing the mushroom parameters. The coupling capacitance (C_o) and inductance (L) can be approximated by the following expressions [11, 21, 22]:

$$C_o = \frac{W_{e1}\varepsilon_o(1+\varepsilon_{eff})}{\pi}\cosh^{-1}\left(\frac{W_{e1}+g}{g}\right), \tag{2}$$

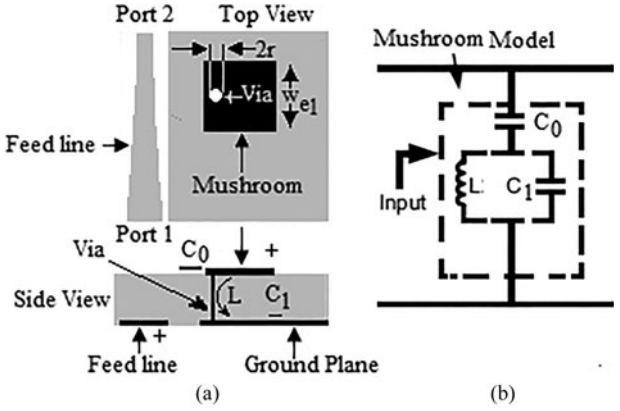

Fig. 3. (a) Configuration schematic view. (b) Equivalent circuit model.

https://doi.org/10.1017/S1759078715001348 Published online by Cambridge University Press

where

$$g \cong d_1 + \frac{(S_1 + S_2)}{2} \text{ and}$$
$$\varepsilon_{eff} = \frac{\varepsilon_r + 1}{2} + \frac{\varepsilon_r - 1}{2}\left(1 + 12\frac{h}{W_{e1}}\right)^{-0.5},$$
$$L = \mu_0 h, \tag{3}$$

where ε_o, μ_o, and ε_{eff} are respectively the permittivity, permeability of free space and effective dielectric constant and g is the gap between the mushroom edge and feed line. The W_{e1} is the width of mushroom cell. For the two-layer circuit board, the capacitance is given by the well-known formula for a parallel plate capacitor. ${W_{e1}}^2$ is the overlap area of the mushroom metal plate and it is separated from ground plane by a substrate height h of dielectric constant ε_r

$$C_1 = \frac{\varepsilon_0 \varepsilon_{eff} {W_{e1}}^2}{h}. \tag{4}$$

III. SIMULATED RESULTS AND DISCUSSION

A) Parametric study and observations

The mushroom of the proposed antenna configuration has been used independently to obtain WiMAX stop band within the UWB frequency region. The notch frequency can be tuned with the variation of any one parameter of the mushroom keeping other parameters constant. Figure 4 shows the variation of voltage standing wave ratio (VSWR) for different width (W_e) of the mushroom. From the characteristics, it is observed that as the width of mushroom patch increases, the notch band shift toward the left side of the plot. This is due to increase of mushroom patch area which is responsible for increasing of capacitance. Thus, the desired notch frequency is controllable by tuning the width of mushroom.

In this paper, both the conventional mushroom type (CM) with via at the center and edge-located via mushroom-type (ELM) [10] toward the feed line for band-notch design are also studied. The ELM has better frequency-rejection function than the CM as is evident from Fig. 5. Compared to a CM antenna, an ELM antenna has a higher VSWR value at the notch frequency and exhibits a better sharp skirt due to better coupling. Therefore, ELM has priority over the CM when it is applied to the design of a UWB band-notched antenna.

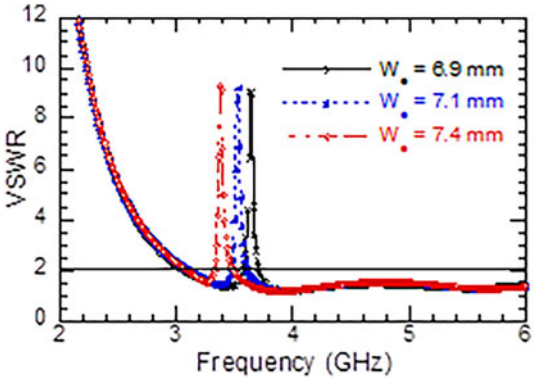

Fig. 4. Variation of VSWR with the variation of width of mushroom patch.

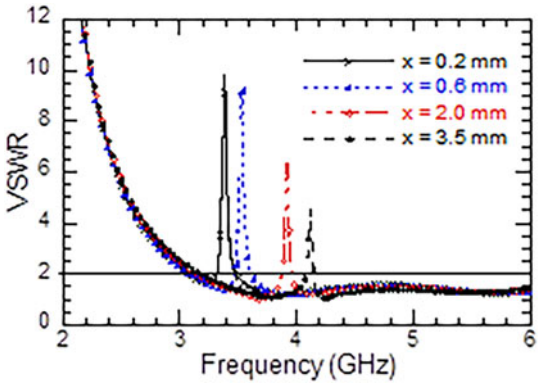

Fig. 5. Variation of VSWR with the variation of via position.

The effect of variation of radius (r) on VSWR plot is shown in Fig. 6. It is clear that as the radius of the via decreases, the center frequency of notch band is also shifted to lower frequency range with some decrease in BW. It is due to the fact that when the radius of via decreases the inductance related to via increases. Thus, via radius has significant effects on the notch band.

Furthermore to realize the WLAN stop band in UWB region a pair of mushroom has been used in the same hexagonal monopole antenna. But, a pair of mushroom cell is used to get the strong frequency rejection characteristics than single cell. The mushroom parameters have enough control on the center notch frequency, width of the rejection

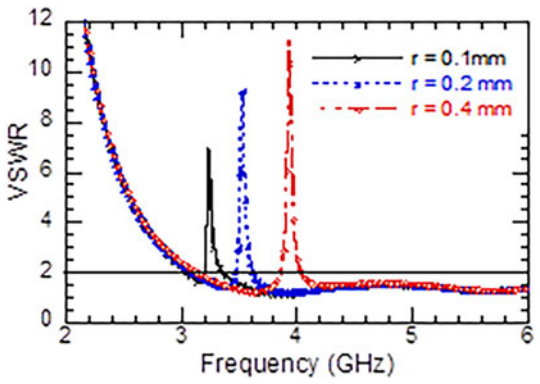

Fig. 6. Variation of VSWR with the variation of via radius r.

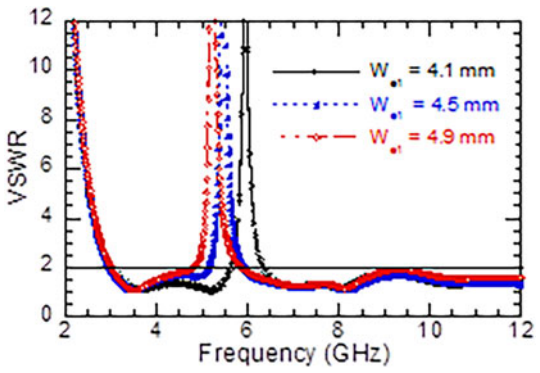

Fig. 7. Variation of VSWR with the variation of width of mushroom patch.

https://doi.org/10.1017/S1759078715001348 Published online by Cambridge University Press

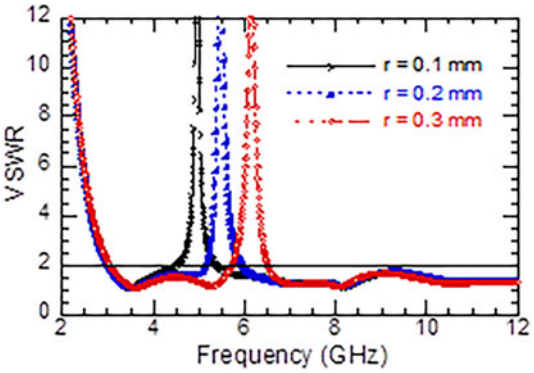

Fig. 8. Variation of VSWR with the variation of via radius *r*.

band as well as the VSWR peak of the desired rejection band as evident Figs 7 and 8. The VSWR curves for all configurations are given in Fig. 9 for comparison. It can be clearly found that each mushroom structure stops a band. Dual narrow notch bands are easily obtained due to the mushroom structures.

B) Input impedance, gain, and efficiency

The real and imaginary parts of input impedance of the proposed antenna are shown in Fig. 10. It is observed that the impedance is mismatch at about 3.5 and 5.5 GHz. This implies that the antenna is stopping the wave at notch frequency which results in steep rise of VSWR. At the notch frequency, most of the power fed into the antenna is reflected back, which leads to a sharp decrease of the antenna gain and efficiency. Simulated gain and efficiency are plotted in Figs 11 and 12, respectively. It is observed that there are two sharp decreases in gain and efficiency at 3.5 and 5.5 GHz, which confirms the effective band-notch operation. However, the proposed antenna has satisfactory gain and efficiency over the whole pass band.

C) Current distribution and analysis

To analyze the band-notch property, the simulated surface current distributions of the proposed antenna at three frequencies are shown in Fig. 13. At a passband frequency of 3.1 and 7.5 GHz, the distribution of surface current is appears at the periphery of the patch (Figs 13(a) and 13(d)), whereas little current appears at the mushroom. This

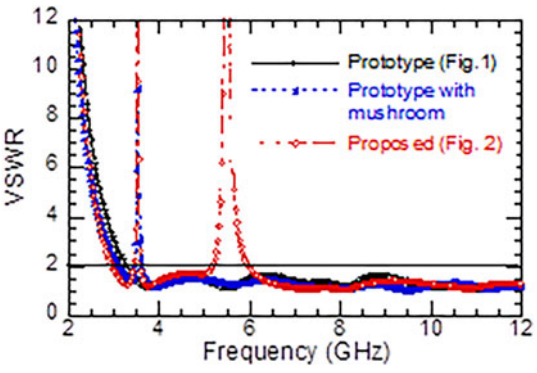

Fig. 9. VSWR characteristics of all configurations for comparison.

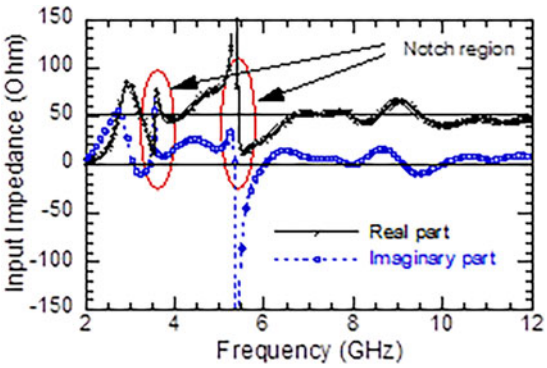

Fig. 10. Simulated input impedance of the proposed antenna.

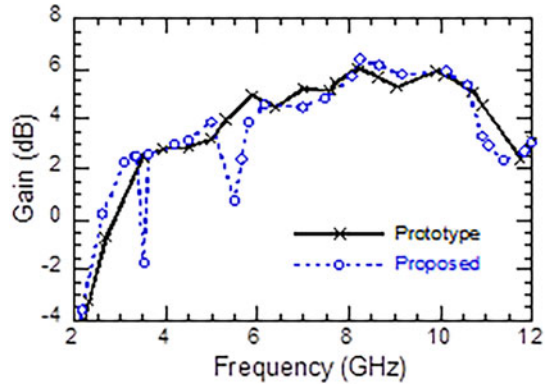

Fig. 11. Simulated gain of the prototype and proposed antennas.

phenomenon indicates the existence of the mushroom with little effect on the UWB antenna. From Figs 13(b) and 13(c), it is observed that the current distribution is concentrated on the mushroom at the notch frequencies. This indicates that the antenna cannot be radiated effectively at the notch bands. Therefore, mushroom stops the surface current and as a result notch bands are obtained.

IV. MEASUREMENT RESULTS

The photographic view of the prototype and proposed antennas are given in Fig. 14. The simulation and tested responses of prototype antenna are shown in Fig. 15. It is clear that the

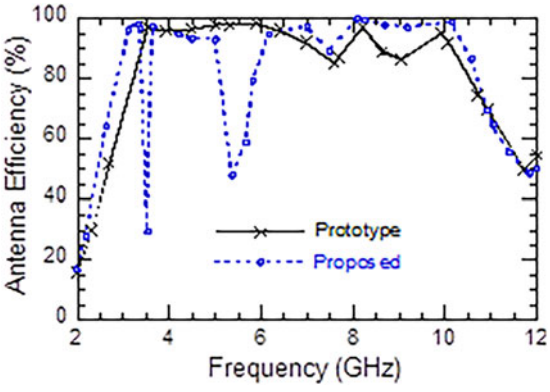

Fig. 12. Simulated efficiency of the prototype and proposed antennas.

https://doi.org/10.1017/S1759078715001348 Published online by Cambridge University Press

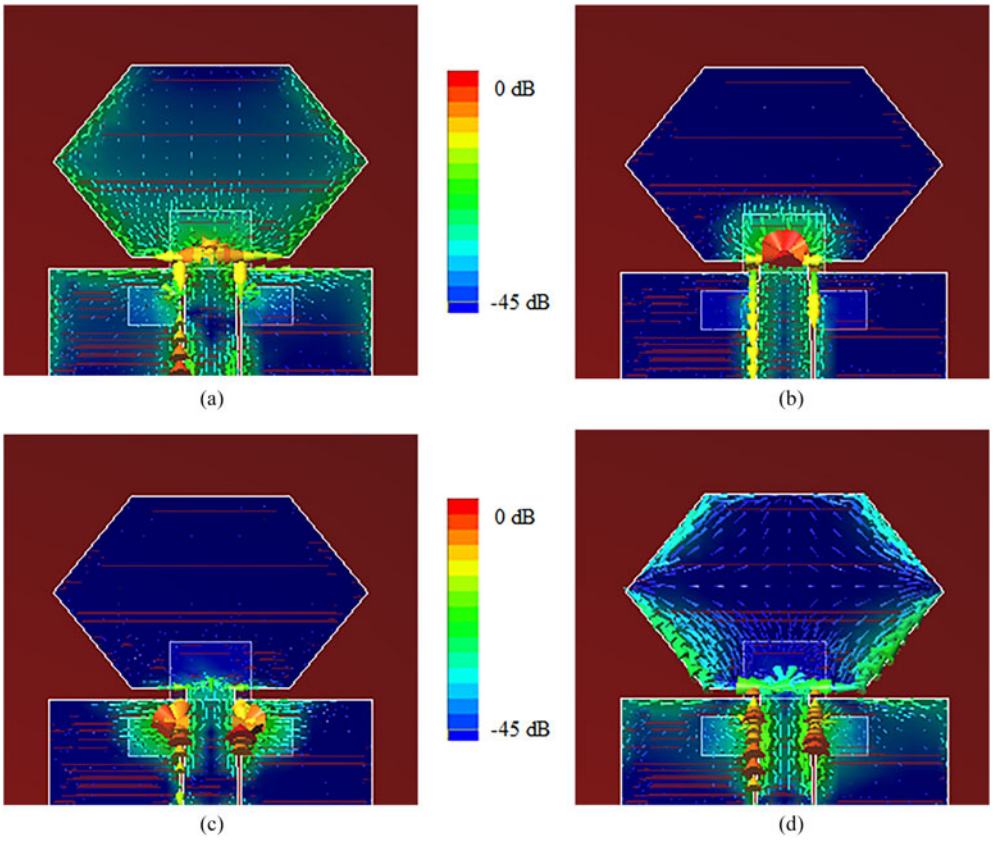

Fig. 13. Surface current distributions on the proposed antenna. (a) 3.1 GHz, (b) 3.5 GHz, (c) 5.5 GHz, and (d) 7.5 GHz.

measured result covers the whole US-FCC-specified UWB operating range. Thus, it may be considered as a good UWB antenna. Figure 16 shows the VSWR characteristics of the proposed antenna for comparison and the results are given in Table 2. The proposed antenna rejects the WiMAX and WLAN bands and still performs good impedance matching over the UWB frequency span. The measured results comply with the simulated results. The dimensional mismatch of fabricated structure and loss tangent of substrate may cause the difference between simulated and measured results.

The antenna is designed in the *X*–*Y* plane and it is *Y*-polarized because the monopole element is in the *Y*-direction. Therefore, the *E*-plane for this antenna is the *YZ*-plane and the *H*-plane is the *XZ*-plane. Figure 17 presents the comparison of the radiation patterns between the prototype and proposed antennas at 3.15 and 8.75 GHz. The radiation patterns of the proposed antenna are more or less same as

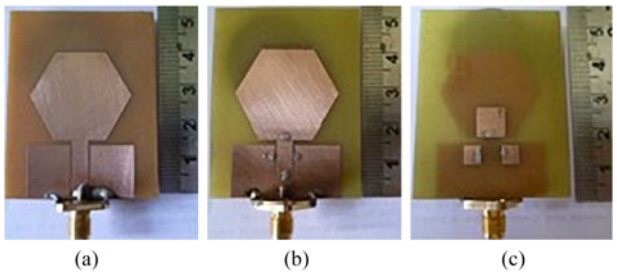

Fig. 14. Fabricated stucture of (a) prototype (top plane), (b) proposed (top plane), and (c) proposed (bottom plane).

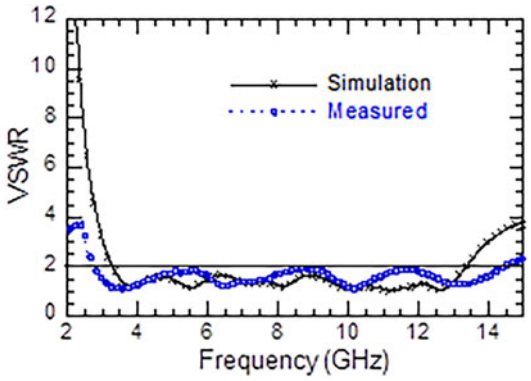

Fig. 15. VSWR versus frequency of prototype antenna.

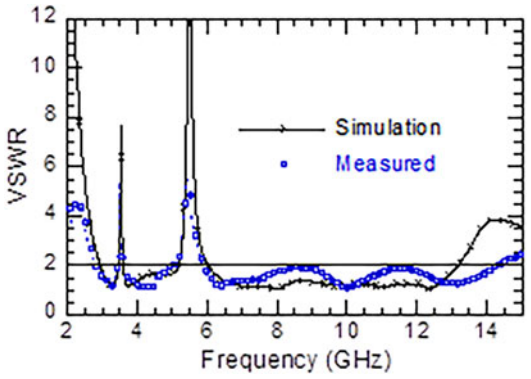

Fig. 16. VSWR versus frequency of the proposed antenna.

https://doi.org/10.1017/S1759078715001348 Published online by Cambridge University Press

Table 2. Comparison of the simulated and measured results (all frequencies in GHz).

Band → / Antenna ↓	UWB		WiMAX		WLAN	
	Lower edge	Upper edge	Lower edge	Upper edge	Lower edge	Upper edge
Prototype (simulated)	3.15	13.40	–	–	–	–
Prototype (measured)	2.77	14.44	–	–	–	–
Proposed (simulated)	2.91	13.19	3.3	3.7	5.15	5.97
Proposed (measured)	2.81	14.32	3.3	3.7	5.10	5.88

the prototype antenna. Thus, the introductions of mushrooms have little effect on the radiation patterns. It can be observed that at the low frequency of 3.15 GHz, the radiation on the E_ϕ versus θ pattern at $\phi = 0^\circ$ plane is omnidirectional, whereas in E_θ versus θ pattern at $\phi = 90^\circ$ plane is figure of eight in shape because of the small ground plane on the same side of the patch. At a higher frequency of 8.5 GHz, the radiation pattern still retains a satisfactory omnidirectional on the $\phi = 0^\circ$ plane over the entire BW in both simulation and measurement. The cross-polar pattern in the H-plane increases as frequency rises due to higher mode excitation by the structure and J_x current at the lower edge of radiating patch near the ground plane. However, the patterns are stable over the whole UWB frequency region except the notch bands.

V. TIME-DOMAIN STUDY

The group delay is able to show any nonlinearity that may be present in the phase response and indicates the degree of the

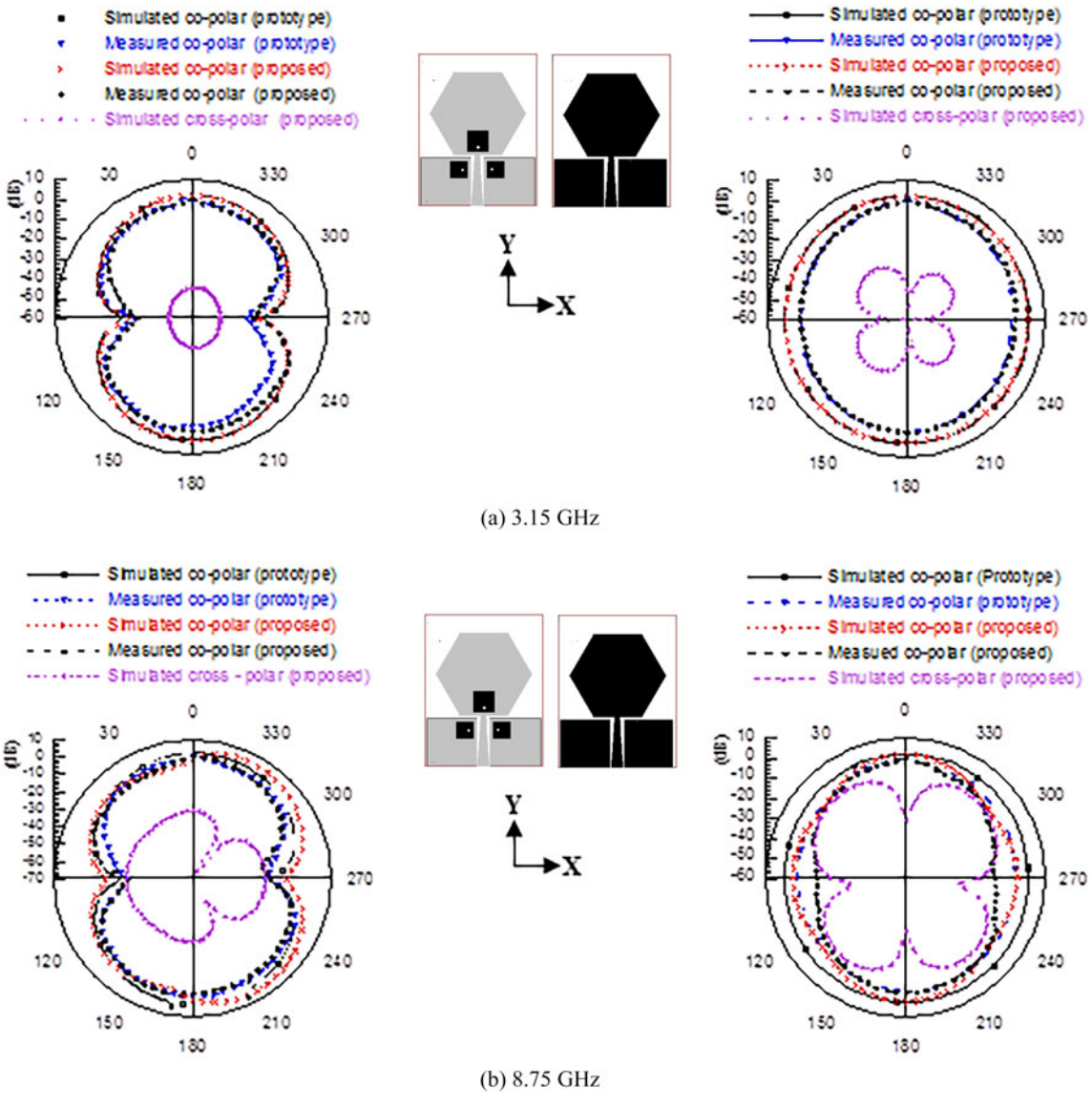

Fig. 17. Simulated and measured radiation patterns.

https://doi.org/10.1017/S1759078715001348 Published online by Cambridge University Press

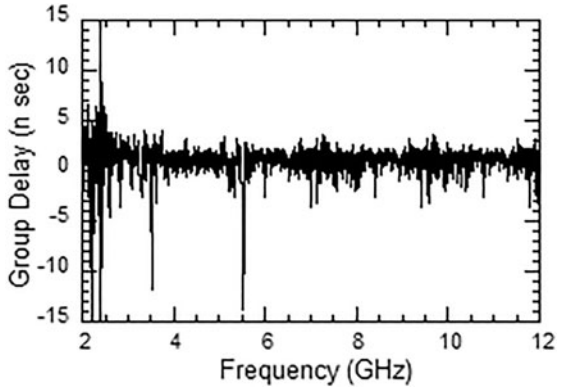

Fig. 18. Measured group delay of the proposed antenna system.

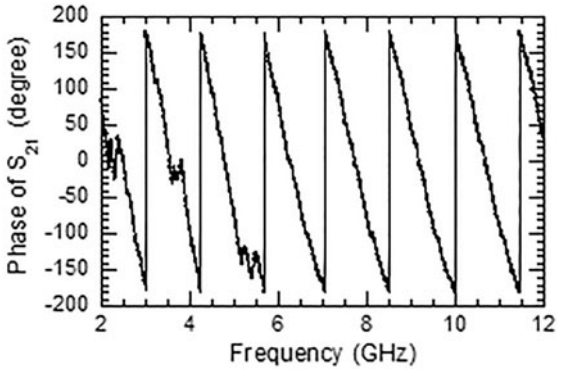

Fig. 19. Measured phase of the proposed antenna system.

distortion. For UWB applications, the phase of the transfer function should be linear as much as possible in the operating band. The group delay is required to be constant over the entire band as well. The group delay of the proposed antenna is shown in Fig. 18. It is measured using a pair of proposed antennas placed at a distance of 160 mm. From Fig. 18, it is observed that the variation of group delay is small across the whole operating band except notch bands. The phase of S_{21} (Fig. 19) is relatively linear within the operating region excluding the notch bands in face to face mode. Thus, the proposed antenna has a good time-domain performance and a small pulse distortion as well.

VI. CONCLUSIONS

A CPW-fed simple UWB antenna with dual stop band has been proposed. The desired stop bands are realized by mushroom structures. The geometric parameters of mushroom offer sufficient freedom for selecting and shifting the desired notch band. The input impedance, conceptual equivalent circuit model, and surface distributions are used to analyze of dual notch bands characteristics. The existences of the mushroom have little effects on the radiation pattern. The measured results comply with the simulated ones. The antenna has constant group delay and linear phase within the operating band except notch bands which ensures the good linear transmission performances. Therefore, the proposed antenna is expected a good candidate for UWB applications.

REFERENCES

[1] First Report and Order. Revision of Part 15 of the Commission's Rule Regarding Ultra-wideband Transmission.

[2] Azim, R.; Islam, M.T.; Mandeep, J.S.; Mobashsher, A.T.: A planar circular ring ultra-wideband antenna with dual band-notched characteristics. J. Electromagn. Waves Appl., **26** (14–15) (2012), 2022–2032.

[3] Li, P.; Liang, J.; Chen, X.: Study of printed elliptical/circular slot antennas for ultra-wide band applications. IEEE Trans. Antennas Propag., **54** (6) (2006), 1670–1675.

[4] Ray, K.P.; Tiwari, S.: Ultra wideband printed hexagonal monopole antennas. IET Microw. Antennas Propag., **4** (4) (2010), 437–445.

[5] Liao, X.J.; Yang, H.C.; Han, N.; Li, Y.: Aperture UWB antenna with triple band-notched characteristics. Electron. Lett., **47** (2) (2011).

[6] Chen, H.; Ding, Y.; Cai, D.S.: A CPW fed UWB antenna with WiMAX/WLAN band notched characteristics. Progress Electromagn. Res. Lett., **25** (2011), 163–173.

[7] Li, W.T.; Hei, Y.Q.: Design of a ultra wide band antenna with multiple band notch characteristics. J. Electromagn. Waves Appl., **26** (2012), 942–951.

[8] Xie, H.H.; Jiao, Y.C.; Chen, L.N.; Zhang, F.S.: Omnidirectional horizontally polarized antenna with EBG cavity for gain enhancement. Progress Electromagn. Res. Lett., **15** (2010), 79–87.

[9] Pirhadi, A.; Hakkak, M.; Keshmiri, F.: Using electromagnetic band gap superstrate to enhance the Bandwidth of probe-fed microstrip antenna. Progress Electromagn. Res., **61** (2006), 215–230.

[10] Makinen, R.; Pynttari, V.; Heikkinen, J.; Kivikoski, M.: Improvement of antenna isolation in hand-held devices using miniaturized electromagnetic band gap structures. Microw. Opt. Technol. Lett., **49** (10) (2007), 2508–2513.

[11] Yazdi, M.; Komjani, N.: Design of a band-notched UWB monopole antenna by means of an EBG structure. IEEE Antenna Wireless Propag. Lett., **10** (2011), 170–173.

[12] Peng, L.; Li Ruan, C.: UWB band-notched monopole antenna design using electromagnetic-bandgap structures. IEEE Trans. Microw. Theory Techn., **59** (4) (2011), 1074–1081.

[13] Xie, J.J.; Yin, Y.Z.; Wang, J.; Pan, S.L.: A novel tri-band circular slot patch antenna with an EBG structure for WLAN/WiMAX applications. J. Electromagn. Waves Appl., **26** (2012), 493–502.

[14] Xu, J.; Miao, C.; Yang, G.; Cui, L.; Zhang, J.D.; Ji, Y.X.; Wu, W.: Compact and sharp rejection microstrip UWB BPF with dual narrow notched bands. J. Electromagn. Waves Appl., **25** (2011), 2464–2474.

[15] Xu, F., Wang, Z.X.; Chen, X.; Wang, X.A.: Dual band-notched UWB antenna based on spiral electromagnetic-band gap structure. Progress Electromagn. Res. B, **39** (2012), 393–409.

[16] Li, T., Zhai, H.Q.; Li, G.H.; Liang, C.H.: Design of compact UWB band- notched antenna by means of electromagnetic- band gap structures. Electron. Lett., **48** (11) (2012).

[17] Li, Y.; Li, W.; Jiang, T.: Implementation and investigation of a compact circular wide slot UWB antenna with dual notched band characteristics using stepped impedance resonators. Radioengineering, **21** (1) (2012), 517–527.

[18] Chattopadhay, K.; Das, S.; Das, S.; Chaudhuri, S.R.B.: Ultrawide performances of printed hexagonal wideslot antenna with dual band notched characteristics. Progress Electromagn. Res. C, **44** (2013), 83–93.

https://doi.org/10.1017/S1759078715001348 Published online by Cambridge University Press

[19] Hongnara, T.; Mahattanajatuphat, C.; Akkaraekthalin, P.; Krairiksh, M.: A multiband CPW-fed slot antenna with fractal stub and parasitic line. Radioengineering, **21** (2) (2012), 597–603.

[20] Mandal, T.; Das, S.: Design of a CPW fed simple hexagonal shape UWB antenna with WLAN and WiMAX band rejection characteristics. J. Comput. Electron., **14** (1) (2015), 300–308.

[21] Cheng, H.R.; Song, Q.Y.: Design of a novel EBG structure and its application in fractal microstrip antenna. Progress Electromagn. Res. C, **11** (2009), 81–90.

[22] Sievenpiper, D.F.: High-Impedance Electromagnetic Surfaces. Ph.D. thesis, University of California, Los Angeles, 1999.

Tapan Mandal (1977) received the B.Tech. degree in Electronics and Communication Engineering from Kalyani Govt. Engineering College of Kalyani University in the year 2001. He has received M.E. degree from Bengal Engineering College (D.U.), Shibpur, India, in the year 2003. From 2004 to 2007, he worked as a Lecturer at the University Institute of Technology, Burdwan University. Since 2007, he is associated with the Department of Information Technology of Govt. College of Engineering and Textile Technology, Serampore, India and presently holds the post of an Assistant Professor. His current research interests include the planar printed antenna and electromagnetic band gap structures.

Santanu Das (1968) received the B.E. degree in 1989 in Electronics and Telecommunication Engineering from Bengal Engineering College of Calcutta University (India) and M.E. degree in 1992 in Microwave Engineering from Jadavpur University, Calcutta. He obtained the Ph.D. (Engineering) degree in 1998 from Jadavpur University. He joined as an Lecturer in the Electronics and Telecommunication Engineering, Department of Indian Institute of Engineering Science and Technology, Shibpur, India in 1998 and presently holds the post of Professor. His current research interests include the microstrip circuits, FSS, antenna elements, and arrays. He is a life member of Institution of Engineers, India and senior member of IEEE.

https://doi.org/10.1017/S1759078715001348 Published online by Cambridge University Press